Evaluation of the functional diffusion map as an early biomarker of time-to-progression and overall survival in high-grade glioma

Daniel A. Hamstra*†, Thomas L. Chenevert†‡, Bradford A. Moffat†‡, Timothy D. Johnson†§, Charles R. Meyer†‡, Suresh K. Mukherji‡, Douglas J. Quint‡, Stephen S. Gebarski‡, Xiaoying Fan‡, Christina I. Tsien*, Theodore S. Lawrence*, Larry Junck¶, Alnawaz Rehemtulla*†‡, and Brian D. Ross†‡‖

Departments of *Radiation Oncology, ‡Radiology, §Biostatistics, and ¶Neurology, and †Center for Molecular Imaging, University of Michigan Medical School, 1150 West Medical Center Drive, Medical Sciences Research Building III, Room 9303, Ann Arbor, MI 48109-0648

Communicated by George F. Vande Woude, Van Andel Research Institute, Grand Rapids, MI, September 23, 2005 (received for review June 14, 2005)

Diffuse malignant gliomas, the most common type of brain tumor, carry a dire prognosis and are poorly responsive to initial treatment. The response to treatment is typically evaluated by measurements obtained from radiographic images several months after the start of treatment; therefore, an early biomarker of tumor response would be useful for making early treatment decisions and for prognostic information. Thirty-four patients with malignant glioma were examined by diffusion MRI before treatment and 3 weeks later. These images were coregistered, and differences in tumor-water diffusion values were calculated as functional diffusion maps (fDM), which were correlated with the radiographic response, time-to-progression (TTP), and overall survival (OS). Changes in fDM at 3 weeks were closely associated with the radiographic response at 10 weeks. The percentage of the tumor undergoing a significant change in the diffusion of water (V_T) was different between patients with progressive disease (PD) vs. stable disease (SD) ($P < 0.001$). Patients classified as PD by fDM analysis at 3 weeks were found to have a shorter TTP compared with SD (median TTP, 4.3 vs. 7.3 months; $P < 0.04$). By using fDM, early patient stratification also was correlated with shorter OS in the PD group compared with SD patients (median survival, 8.0 vs. 18.2 months; $P < 0.01$). On the basis of fDM, tumor assessment provided an early biomarker for response, TTP, and OS in patients with malignant glioma. Further evaluation of this technique is warranted to determine whether it may be useful in the individualization of treatment or evaluation of the response in clinical protocols.

diffusion MRI | human glioma | treatment assessment | surrogate marker

Malignant gliomas [World Health Organization (WHO) grade III/IV] represent a heterogeneous group of tumors, which typically respond poorly to most therapies (1). Until recently, many decades of clinical research failed to offer significant improvement in survival despite the aggressive combination of surgical resection, radiotherapy, and chemotherapy. The response to therapy has typically been assessed 4–6 weeks after the completion of radiation treatment on the basis of the "crossed-diameter product" (CDP) obtained from computed tomography or MRI images (2). Changes in the CDP have been correlated (3–5) with increased survival for patients with high-grade gliomas treated with primary radiation therapy. The radiographic response has also been evaluated after salvage chemotherapy in which an association between response and survival was found in some studies (6, 7) but not in others (8). In all of these analyses, however, efficacy was assessed weeks to months from the start of treatment; therefore, an early biomarker of tumor response might enable earlier clinical decisions to guide care and enable patients to begin second-line therapy sooner, potentially with better performance status (1).

Diffusion MRI, a technique that measures the mobility of water within tissues at the cellular level, has been demonstrated in preclinical models of glioma to be a sensitive and early indicator of both response to therapy and overall survival (OS) (9–13). In these preclinical settings, diffusion MRI was used to measure the therapeutic dose-dependent increase in the mobility of water after cellular death and was shown both to accurately discriminate between different treatment modalities (10, 11) and to predict regional differences in response to therapy (12, 13). The application of diffusion MRI, based on the mean change in the apparent diffusion coefficient (ADC) within the entire tumor, has also been reported in a preliminary series of primary brain tumors or brain metastasis (10, 14), where in 8 separate patients, a correlation between early changes in diffusion and later radiographic response was observed (14). However, the bulk of these patients had metastatic disease, with only one patient with a primary high-grade glioma, and no analysis of the patient progression or survival was reported; therefore, the general applicability of this technique remains to be seen.

Alterations in the tumor after therapy may involve cell swelling (secondary to loss of cellular water homeostasis), followed by subsequent necrosis or apoptotic-induced cellular death. In addition, there may be a reorganization of free extracellular water as seen for edema or cystic regions. The interplay of all of these factors may produce transient, spatially varying decreases and increases in regional diffusion values, which may be underestimated by using the mean ADC. In contrast, functional diffusion maps (fDM) have been developed in which regional variations in diffusion (both increasing and decreasing) can be quantified. When applied to a population of patients with a heterogeneous mix of primary brain tumors 3 weeks after the start of treatment, this fDM approach was found to accurately predict the response several months later (15). The purpose of this study was to discover whether fDM analysis of the treatment response, limited to a more homogenous population of patients with high-grade glioma, would prove to be an early biomarker for response, time-to-progression (TTP), and OS.

Methods

Patients. Patients treated at the University of Michigan Medical Center with pathologically proven primary brain tumors were eligible for enrollment on a protocol using diffusion-weighted imaging to evaluate the treatment response. Between February 1999 and September 2004, 54 patients were enrolled in this study;

Conflict of interest statement: T.L.C., A.R., and B.D.R. have a financial interest in the underlying technology (patent no. 6,567,684) discussed in this article. Furthermore, this technology is licensed to Molecular Theraputics, Inc. in which A.R. and B.D.R. have a financial interest.

Freely available online through the PNAS open access option.

Abbreviations: WHO, World Health Organization; CDP, crossed-diameter product; OS, overall survival; ADC, apparent diffusion coefficient; fDM, functional diffusion map; TTP, time-to-progression; PR, partial response; SD, stable disease; PD, progressive disease; C.I., confidence intervals; AUC, area under the curve; RPA, recursive partition analysis.

‖To whom correspondence should be addressed. E-mail: bdross@umich.edu.

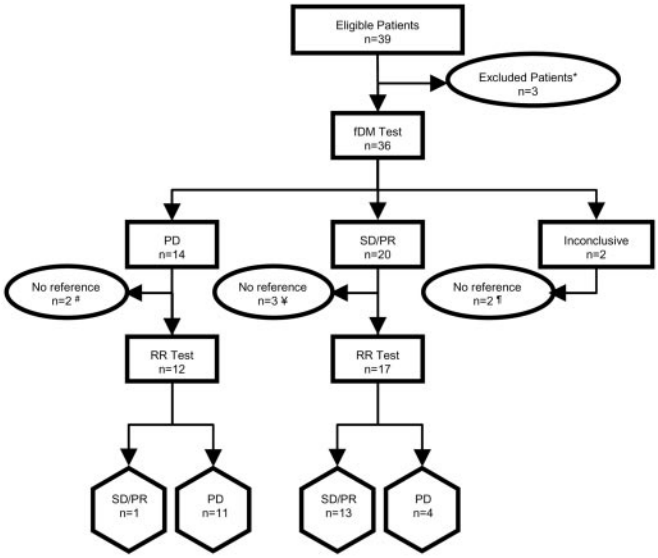

Fig. 1. Flow diagram of patient categorizations. Thirty-nine patients with grade III/IV glioma were enrolled. SD, stable disease; PD, progressive disease; PR, partial response; RR, radiographic response by MRI. *, Three patients did not undergo MRI scans, including one patient who entered hospice without receiving adjuvant therapy, one patient who declined further participation, and one patient who had claustrophobia and could not tolerate the MRI procedure. #, Two patients stratified as PD by fDM did not have radiographic follow-up at 10 weeks, including one who died secondary to neutropenia and sepsis and one who did not receive the first posttreatment scan until week 22. ¥, Three patients stratified as SD/PR by fDM did not have radiographic follow-up at 10 weeks, including one patient who died at 6 weeks before radiographic evaluation, one who was lost to follow-up, and one who had salvage surgery shortly after completing radiotherapy. ¶, Two patients had large cystic lesions requiring the insertion of a catheter and frequent aspiration of fluid, which made their scans nondiagnostic both by fDM and by CDP.

of these patients, 39 had a diagnosis of diffuse high-grade glioma (WHO grade III or IV) of the cerebral hemispheres and form the basis of this study. Written, informed consent was obtained from subjects, and all images and medical records were obtained according to protocols approved by the University of Michigan Medical School Institutional Review Board.

Of the 39 patients with high-grade glioma enrolled in the trial, 36 were able to undergo both the pretreatment and the 3-week panel of scans, including diffusion MRI as well as the standard 1.5-T MRI exams (fluid-attenuated inversion recovery MRI, T2-weighted MRI, and gadolinium-enhanced T1-weighted MRI) (see Fig. 1 for details). Twenty-nine of these 36 patients had a usable radiographic follow-up at 10.0 ± 0.2 weeks (median ± SEM) to compare fDM with radiographic response. Five patients did not have MRI scans at 10 weeks and were, therefore, not used to compare fDM and radiographic response but were included for all survival analysis on the basis of their fDM categorization at 3 weeks. Analysis by fDM could not be performed on two patients who had large cysts requiring the insertion of catheters and the frequent drainage of fluid. Therefore, 34 patients were studied for analysis of TTP and OS (see Fig. 1). Eleven of these patients were included in our previous fDM analysis (15).

Radiographic Scans. Patients underwent scans 1 week before treatment, 3 weeks after the start of treatment, and 4–6 weeks after the end of treatment. Routine clinical follow-up scans were generally obtained every 2–3 months. For fDM analysis, pretreatment scans were obtained an average of 5.2 ± 0.6 days (mean ± SEM) before the start of treatment, and the follow-up scan was obtained 3.1 ± 0.1 weeks (mean ± SEM) after the start of treatment.

End Points. The three end-points analyzed in this study were the radiographic response at 10 weeks after the start of treatment, OS, and TTP. The radiographic response at 10 weeks after the initiation of therapy was based on steroid doses and the CDP on T1 contrast-enhanced MRI and classified according to the following WHO criteria: a complete response, partial response (PR), stable disease (SD), and progressive disease (PD) (2). To assess the effect of steroids on the radiographic response, steroid doses were recorded before each scan, weekly during radiotherapy, and at each follow-up.

Treatment. Radiotherapy was administered at the University of Michigan Medical Center or one of its off-campus facilities by using 3D-conformal therapy with ≥6-MV photons. Treatment was performed by using standard techniques, which typically involved a 2.0–2.5-cm margin on either the enhancing region on the T1 gadolinium-enhanced scans or the abnormal signal on the T2-weighted scans to 46 Gy in 2-Gy fractions followed by subsequent shrinking fields to a final median dose of 70 Gy (see Table 1) (16). Chemotherapy was most often provided in the adjuvant setting and was at the discretion of the treating physician (see Table 1).

MRI. Diffusion imaging was accomplished on a 1.5-T human MRI system (General Electric) by using a single-shot, spin-echo, diffusion-sensitized, echo-planar imaging acquisition sequence. The echo-planar imaging sequence (TR/TE = 10,000/100 ms) was set to acquire at least 24, 6-mm-thick, contiguous axial-oblique sections through the brain at given diffusion sensitivities (i.e., "*b* factors") along all three orthogonal directions. A set of diffusion-weighted images at high diffusion sensitivity (b_1 = 1,000 s/mm^2) and low sensitivity ($b_0 \approx 0$ s/mm^2; i.e., T2-weighted) were collected in 40 s. The diffusion-weighted images for the three orthogonal directions and b_0 image were combined to calculate an ADC map (17). ADC calculated in this manner is rotationally invariant and, thus, is independent of the diffusion anisotropy known to exist in neural tissues (18). The fDMs were calculated from the ADC images, as reported in ref. 15; this technique is briefly outlined below.

fDM Analysis. All magnetic resonance images were coregistered to the initial pretreatment magnetic resonance images with an automated mutual information module (19). After this coregistration, brain tumors were manually contoured on the images by radiologists who defined the regions of interest on the enhancing areas on the contrast-enhanced T1-weighted images. The ADC values of each voxel within the tumor at week 3 were compared with the pretherapy values. Shrinkage or growth of the tumor during the time between scans may have occurred; therefore, only voxels that were present in both the pretherapy and posttherapy tumor volumes were included. The tumor was further segmented into three different categories, yielding the fDMs in which the red voxels represent areas within the tumor where ADC increased ($>55 \times 10^{-5}$ mm^2/s), the blue voxels represent a decreased ADC ($<55 \times 10^{-5}$ mm^2/s), and the green voxels represent regions within the tumor that were within these thresholds. The basis for these thresholds was described in ref. 15. Briefly, the thresholds were empirically determined to be the 95% confidence intervals (C.I.) (or 1.96× the standardized residual) calculated from normal contralateral brain tissues, including white matter, gray matter, and cerebrospinal fluid. The percentage of the tumor within these three categories was then calculated as V_R, V_B, and V_G, respectively, and the total percentage of the tumor with a significant change (V_R + V_B) in the diffusion values was calculated as V_T.

Statistical Analysis. The thresholds for determining whether detectable fDM changes (V_R, V_B, and V_T) were correlated with the radiographic response and were determined empirically for a total of 29 patients by using receiver operator curve analysis. These patients were selected because they had a complete set of coreg-

Table 1. Characteristics of patient population

Factor	Group	PD	SD/PR	*P**
Total sample size	34	14 (41)	20 (59)	
Age, years				>0.1†
Median	54 (20–75)	55 (20–73)	51 (23–75)	
Gender				>0.1‡
Male	13 (38)	9 (45)	4 (29)	
Female	21 (62)	11 (55)	10 (71)	
Pathology				>0.1‡
WHO grade III	7 (21)	3 (21)	4 (20)	
WHO grade IV	27 (79)	11 (79)	16 (80)	
Karnofsky performance status				>0.1‡
≥70	24 (71)	11 (79)	13 (65)	
<70	10 (29)	3 (21)	7 (35)	
Surgery				0.09‡
Biopsy	17 (50)	10 (71)	7 (35)	
Surgical resection	17 (50)	4 (29)	13 (65)	
Tumor location				>0.1‡
Frontal	10 (29)	3 (21)	7 (35)	
Parietal	8 (24)	3 (21)	5 (25)	
Temporal	9 (26)	4 (29)	5 (29)	
Thalamic	6 (18)	4 (29)	2 (10)	
Multifocal	1 (3)	1 (5)		
Radiation therapy				>0.1‡
Yes	33 (97)	13 (93)	20 (100)	
No	1 (3)	1 (7)		
Median dose, Gy	70 (0–75)	70 (0–75)	70 (36–75)	>0.1†
Chemotherapy				>0.1‡
Yes	29 (85)	13 (93)	16 (80)	
No	5 (15)	1 (7)	4 (20)	
Concurrent TMZ/XRT	8 (24)	2 (14)	6 (30)	>0.1‡
Any TMZ	28 (82)	12 (86)	16 (80)	

Entries are number (and range or percentage) in each category. TMZ, temozolomide; XRT, radiation therapy.
**P* refers to the differences between the columns SD/PR and PD.
†Student's *t* test.
‡Fisher's exact test.

istered images available for which pretreatment, 3 week, and 10 week scans were available. Given this small population of patients, both training and test sets were not deemed possible to validate fDM predictions of the radiographic response at 10 weeks; therefore, cross-validation (leaving one out at a time) was performed for fDM, mean ADC, and changes in CDP at 3 weeks compared with the radiographic response at 10 weeks. Cross-validation is one of the simplest and most widely used methods for estimating prediction error. However, a training population was not possible on this size data set; therefore a leave-one-out cross-validation was used because it is an unbiased estimate for prediction error (20). All statistical analysis was done by using MEDCALC V.8.0 (MedCalc Software, Mariakerke, Belgium). Differences between groups were assessed on the basis of categorical variables by using Fisher's exact test, whereas differences between groups with continuous variables were performed by using Student's *t* test. Single-covariate survival analysis was performed by using the log-rank test, and step-wise forward Cox proportional hazards models were used for multivariable survival analyses. In addition, the RPA analysis was performed on 33 of 34 patients. One patient was treated at recurrence and was not included in the RPA analysis.

Results

Patient Characteristics. A total of 34 patients with malignant glioma were enrolled in this study and available for analysis (Table 1). Twenty-seven patients had glioblastoma multiforme (WHO grade IV), and seven had anaplastic astrocytoma (WHO grade III). There were no significant differences in the distribution of either the known prognostic factors or treatments between those patients subsequently defined as PD by fDM vs. those defined as either having SD or PR. There was a trend toward more frontal/parietal tumors in the group stratified as SD/PR and more temporal/thalamic tumors in the group stratified as PD; however, this difference did not achieve statistical significance ($P > 0.05$). Median follow-up for all patients was 10.8 months; for all patients still alive, median follow-up was 12.8 months (range, 8.1–47.3 months). Median OS was 11.9 months, and median TTP was 5.1 months.

fDM Analysis. Fig. 2 *A–C* illustrates representative examples of fDM images overlaid on the T2-weighted images from three patients with glioblastoma multiforme treated with fractionated radiation therapy (total dose, 66–75 Gy) and either adjuvant or concurrent temozolomide therapy (range, 6–16 cycles). These three patients were classified as PD (Fig. 2*A*), SD (Fig. 2*B*), and PR (Fig. 2*C*) on the basis of WHO criteria at 10 weeks. The red, green, and blue voxels/datapoints in these images and the associated scatter plots (Fig. 2 *D–F*) represent the three different tumor regions based on the fDM analysis of ADC change. The percentage of the tumor falling into each of these regions was then used to calculate the three fDM parameters: V_R, V_B, and V_T. In the examples shown, the patient with PD (Fig. 2 *A* and *D*) had a V_T value of only 6% at 3 weeks, whereas the tumor expanded by 56% at 10 weeks. The patient with SD (Fig. 2 *B* and *E*) had a V_T value of 19%, which was predominantly derived from V_B, and a tumor that shrank by 8% at 10 weeks. The patient with a PR (Fig. 2 *C* and *F*) had a large increase in V_T (22%), which was entirely derived from V_R, whereas large changes in V_R were demonstrated (15) to correlate with PR

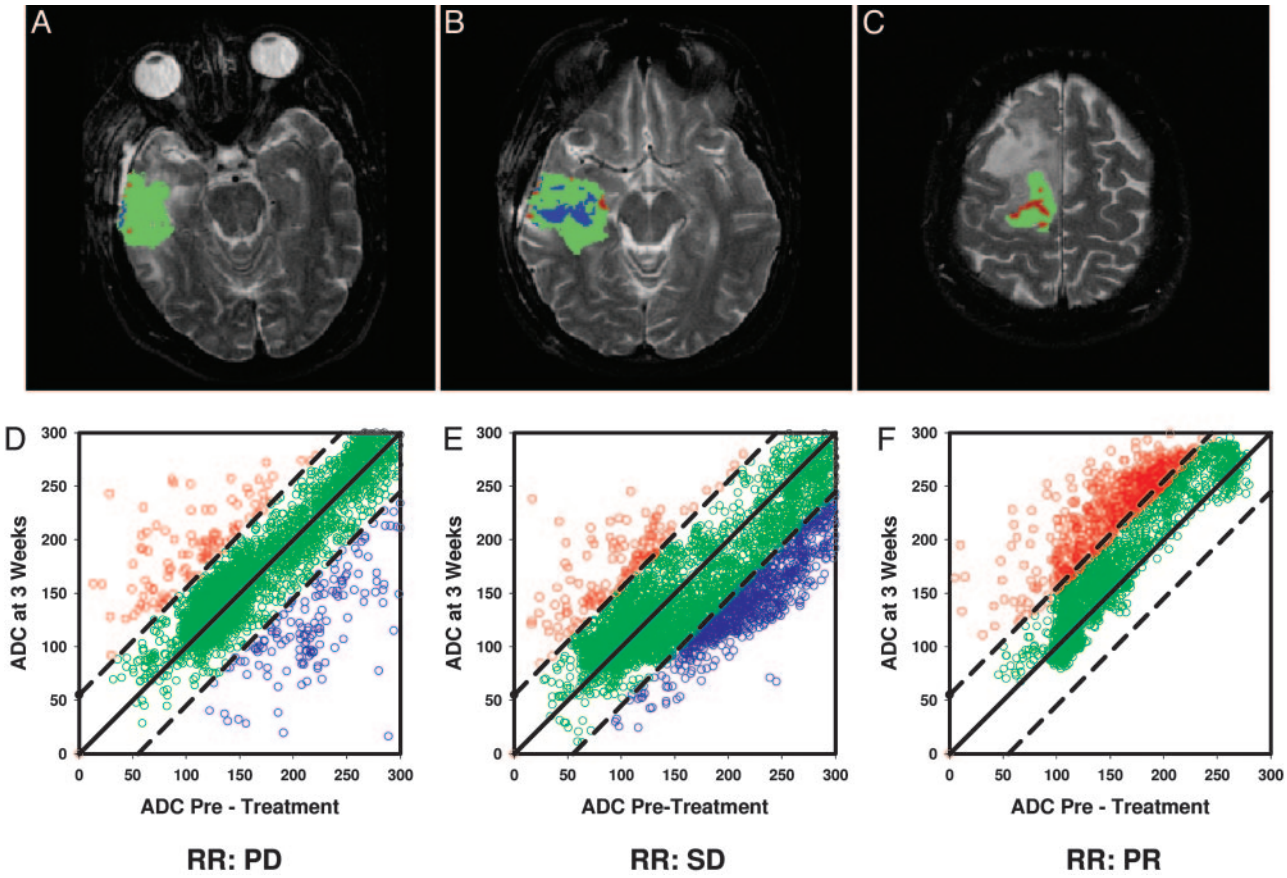

Fig. 2. MRI of three patients with glioblastoma multiforme. Magnetic resonance images were obtained from three representative patients. Images shown are at 3 weeks into a 7-week fractionated radiation regimen. Regions of interests were drawn for each tumor image by using anatomical images. (*A–C*) The regional spatial distributions of ADC changes (fDMs) in a single slice from each tumor are shown as color overlays for a PD (*A*), SD (*B*), and PR (*C*) patient. The red pixels indicate areas of increased diffusion, whereas the blue and green pixels indicate regions of decreased and unchanged ADC, respectively. (*D–F*) The scatter plots quantitatively show the distribution of ADC (1×10^{-5} mm^2/s) changes for the entire 3D tumor volume, whereas radiographic response (RR) labels are given at the bottom, indicating each patient's WHO-based classification at week 10. (*A* and *D*) A patient with progressive disease at 10 weeks and fDM parameters of $V_R = 2.8$, $V_B = 3.2$, and $V_T = 6.0$. (*B* and *E*) A patient with SD at 10 weeks and fDM parameters of $V_R = 2.5$, $V_B = 16.5$, and $V_T = 19.0$. (*C* and *F*) A patient with a partial response at 10 weeks and fDM parameters of $V_R = 22.1$, $V_B = 0$, and $V_T = 22.1$.

patients and a tumor that was 70% smaller on radiographic follow-up.

Correlation of fDMs with Radiographic Response. The radiographic follow-up of the tumor response was performed at 10.0 ± 0.2 weeks (mean ± SEM) from the start of treatment and was available for 29 of 34 patients, yielding: PD in 15 (52%), SD in 12 (41%), and PR in 2 (7%). No complete responses to therapy were identified. Fig. 3 summarizes the percentage of tumors exhibiting the representative changes in V_R, V_B, and V_T at 3 weeks, as stratified by their radiographic response at 10 weeks. In pair-wise comparison, V_R, V_B, and V_T percentages were different between PD and SD ($P < 0.05$ for each; Student's *t* test). Given that only two patients had PR, we combined this group with the SD patients for further analysis (SD/PR). Patients with radiologic PD at 10 weeks had $V_R = 2.6 \pm 0.9\%$ (mean ± SEM) at 3 weeks after treatment initiation, which was half that for SD/PR ($V_R = 6.4 \pm 1.5\%$; $P = 0.04$) (Fig. 3*A*). Similarly, the PD group had $V_B = 3.1 \pm 0.9\%$ (mean ± SEM) at 3 weeks, which was significantly different when compared with SD/PR ($V_B = 11.4 \pm 2.9\%$; $P = 0.01$) (Fig. 3*B*). Finally, the sum of the total diffusion changes ($V_T = V_R + V_B$) for PD was 5.7 ± 1.4%, which had the greatest separation from SD/PR (17.8 ± 2.7%; $P < 0.001$) (mean ± SEM) (Fig. 3*C*).

Receiver operator curve analysis of these three fDM parameters (V_R, V_B, and V_T) compared with the radiographic response revealed a V_T threshold of ≤6.57% as the most predictive of progression by using cross-validation [sensitivity, 75% (95% C.I., 45–92) and specificity, 93% (95% C.I., 66–99)]. V_T at 3 weeks was also a better

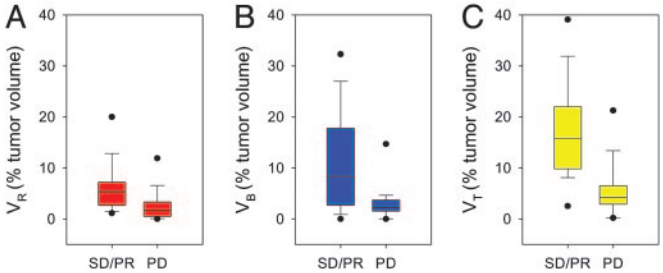

Fig. 3. Box plots summarizing fDM tumor volumes as a percentage of total tumor volume for each patient group, PD ($n = 15$) and SD/PR ($n = 14$). (*A*) The volumes (percentage of total) within the tumors that experienced significantly increased diffusion values (V_R). (*B*) The results for the tumor volumes that had a significant decrease in diffusion values (V_B). (*C*) The total volume of tumors that had any significant change in ADC (V_T, where $V_T = V_R + V_B$). Values depicted are the median for each group with the upper and lower limits of the box representing the 75th and 25th percentile, respectively. The error bars represent the 95th and the 5th percentiles. The dots are the limits (maximum and minimum) of the data range. *P* values (Student's *t* test, unpaired, two-tailed, and unequal variance) $V_R = 0.04$, $V_B = 0.01$, and $V_T < 0.001$.

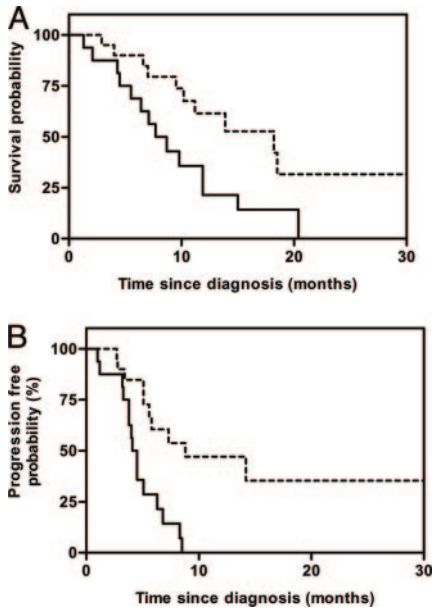

Fig. 4. OS and TTP as a function of fDM stratification at 3 weeks. (*A*) The Kaplan–Meier survival plot of OS for patients stratified as SD/PR ($n = 20$; dashed line) with a median survival of 18.2 months vs. those stratified as PD ($n = 14$; solid line) with a median survival of 8.2 months [$P = 0.008$; log-rank test; hazard ratio = 2.6 (95% C.I., 1.2–6.8)]. (*B*) The Kaplan–Meier analysis of TTP for patients stratified as SD/PR ($n = 20$; dashed line) with a median TTP of 7.3 months vs. those stratified as PD ($n = 14$; solid line) with a median TTP of 4.3 months [$P = 0.03$; log-rank test; hazard ratio = 3.2 (95% C.I., 1.9–11.2)].

predictor of PD than the mean ADC or the CDP measured at the same 3-week time point, as exhibited by a greater area under the curve (AUC) after receiver operator curve analysis (V_T, AUC = 0.83) than either the change in crossed-diameter (AUC = 0.66) or mean ADC (AUC = 0.75). On a patient-by-patient analysis, the V_T threshold correctly identified 13 of 14 stable or responsive tumors (SD/PR) and 11 of 15 progressive tumors (PD). The complete breakdown of patients according to the standards for reporting for diagnostic accuracy are depicted in Fig. 1 (21).

fDM Categorization Correlated with OS and TTP. To assess the correlation of fDM analysis with patient outcome, all 34 patients with 3-week data available were categorized as either PD or SD/PR on the basis of the V_T threshold, as indicated above. The log-rank test and Kaplan–Meier curves revealed that PD at 3 weeks by fDM greatly increased the risk for both death (hazard ratio = 2.6; 95% C.I., 1.2–6.8) (Fig. 4*A*) and progression (hazard ratio = 3.2; 95% C.I., 1.9–11.2) (Fig. 4*B*). Patients identified as PD 3 weeks into therapy had a shorter median survival (8.2 months) compared with those with SD/PR (18.2 months; $P < 0.01$; log-rank test). Similarly, TTP was also shorter in the PD group (4.3 months) vs. those in the SD/PR groups (7.3 months; $P < 0.04$; log-rank test).

Single-covariate analysis of the commonly observed prognostic factors in high-grade glioma [age (<50 vs. ≥50), pathology (grade III vs. grade IV), and extent of surgery (surgical resection vs. biopsy)] revealed that a younger age, pathologic grade III, and surgical resection all exhibited a trend toward increased OS, although none of these achieved statistical significance (all P values were >0.05) (1, 22). The initial location of the tumor (frontal, parietal, temporal, or thalamic) did influence OS ($P < 0.02$) but not TTP ($P > 0.05$). Patients with frontal or parietal tumors had longer survival median survival (17.4 months) than those with either temporal (11.4 months) or thalamic (5.8 months) tumors. The pathologic grade also exhibited a trend toward longer TTP, which also did not achieve statistical significance ($P > 0.1$). Karnofsky performance status (<70 vs. ≥70) did not seem to have prognostic importance in this data set for either OS or TTP.

Table 2. Recursive partition analysis

Group	No. of patients	
	SD/PR	PD
I	1	1
II	0	0
III	4	3
IV	10	4
V	3	4
VI	1	2
Predicted median OS, months	11.1	11.1
Observed median OS, months	18.2	8.0

Roman numerals represent the six partitions, and the arabic numbers correspond to the number of patients per partition. RPA was done using a model described in ref. 22.

By using a multivariate Cox proportional hazards model incorporating age, pathologic grade, extent of surgical resection, tumor location, and fDM, we found that fDM was the only factor predictive of OS ($P < 0.02$). Similarly, in a model for TTP incorporating the same factors, the presence of grade IV as opposed to grade III pathology was an adverse factor for TTP ($P < 0.03$), as was PD documented on 3-week fDM analysis ($P < 0.05$).

A number of studies have evaluated recursive partition analysis (RPA) to stratify patients according to pretreatment variables. RPA for this population of patients (by using the model proposed by Curran *et al.* in ref. 22) revealed no significant differences in the distribution of patients between partitions in the groups categorized as PD or SD/PR; both groups also had predicted median survivals that were identical at 11.1 months ($P > 0.1$) (Table 2). RPA was not predictive of survival in the whole cohort of 33 patients ($P > 0.1$; log-rank test); however, it was predictive for those 27 patients with grade IV tumors ($P = 0.05$). When both RPA and fDM analysis were included in a multivariate Cox proportional hazards model only fDM ($P < 0.04$) but not RPA ($P > 0.1$) had predictive value. Therefore, the ability of fDM to predict early response to therapy is not solely limited to those subjects who would be anticipated to have better survival based on pretreatment factors. Finally, lending further evidence to the validity of fDM as a biomarker, when analyzed as a continuous variable, each incremental increase in V_T was associated with a decreasing hazard ratio for death ($P = 0.05$).

Discussion

These data provide clear evidence that fDM analysis can provide a meaningful early assessment of the treatment response in patients with high-grade glioma and that fDM stratification of tumor response is correlated with both TTP and OS. This association was preserved even when other known prognostic factors were taken into account. In addition, pretreatment ADC alone did not correlate with survival, whereas the changes in diffusion in response to therapy, as measured by fDM, did predict both OS and TTP. In this study, changes in the diffusion of water in response to therapy were evaluated by using fDM. Regions of increased diffusion (red voxels) within the tumor after treatment are associated with a loss of tumor cellularity (10). Moreover, regional decreases in diffusion values were also detected (blue voxels), indicating that a net reduction of extracellular water had occurred in those regions. This decrease has been proposed to be due, in part, to therapeutic-induced cell swelling leading to a decrease in extracellular space (15).

The radiologic tumor response, based on computed tomography or MRI, has been demonstrated (3–5) to offer individual prognostic information to patients being treated with radiotherapy. Unfortunately, this evaluation typically required 5–7 weeks of therapy followed by 3 days to 9 weeks of follow-up, which is a significant

period to wait for an evaluation of treatment efficacy, especially in a population of patients with a median survival of <52 weeks. The presence of stable or nonprogressive disease was a favorable prognostic factor for OS in all three studies (3–5), a finding which was similar to that found with fDM-based predictions made only 3 weeks after treatment initiation.

Recently, a multiinstitutional phase III trial of radiotherapy administered with concurrent and adjuvant temozolomide compared with standard radiotherapy alone (23) provided the first significant improvement in the survival of patients with glioblastoma multiforme in many years. A companion analysis (24) also revealed that a subgroup of patients with methylation and silencing of the O^6-methylguanine-DNA methyltransferase gene appeared to have benefited the most from this treatment. Eight patients in our cohort were treated with temozolomide concurrent with radiation followed by adjuvant temozolomide, making any assessment of this subgroup limited; however, six of these eight subjects were categorized as SD/PR at 3 weeks compared with two subjects with PD (see Table 1). In addition, when these 8 patients were compared to the entire pool of 26 patients treated without the use of concurrent temozolomide, there was a trend toward increased OS ($P = 0.06$; log-rank test). Thus, fDM analysis seems to confirm the results of this treatment modality and may be a useful tool for future clinical trial evaluation.

The pathology of malignant glioma is diverse, with many genetic modifications identified that contribute to its development, and some of these alterations [like those changes seen in recent experience with temozolomide and radiation (24, 25)] probably carry prognostic value. For example, the identification of genetic alterations in oligodendrogliomas in which the 1p and 19q deletions are predictive of the response to chemotherapy is already affecting the care of that disease (26). Given the heterogeneity of high-grade gliomas both between patients and even within the same tumor, however, finding uniform genetic markers to predict response will probably be very challenging; such markers are not readily available at this time (1, 27).

Although these genetic assays are still being developed, predicting the response based on fDM analysis may be applicable across many different primary brain tumors and may add further information to that gained based on pretreatment variables or genetic analysis. Currently, most modern MRI scanners have diffusion protocols as a standard part of their operation, and indeed, "high *b* value" diffusion-weighted imaging has become a mainstay in the evaluation of stroke (28). The time required for diffusion scans would add only 30–60 s to the standard MRI evaluation in addition to a single scan at 3 weeks into the treatment, which is not normally part of clinical practice.

In conclusion, fDM-mediated assessment of early treatment efficacy in high-grade glioma appears very promising. Certainly, a larger group of patients needs to be assessed by using fDM before its true clinical utility can be identified. However, fDM offers the potential to evaluate differences in efficacy between patients, as well as the potential to assess the heterogeneity of response within an individual tumor. For example, fDM analysis could be implemented in an adaptive radiotherapy protocol for glioma by using the early evaluation of the treatment response, which would allow for tailoring treatment between patients or even within individuals. In addition, extension of fDM analysis of tumors outside the brain, including breast lesions (29), rectal carcinoma (30), uterine fibroids (31), prostate (32), tumors of the head and neck (33), and liver metastases (34), as well as whole body diffusion MRI scanning (35) is feasible. Therefore, fDM analysis may be applicable to common malignancies as a tool for monitoring therapeutic efficacy and eventually individualizing patient management on the basis of a real-time evaluation of cellular response.

This work was supported by National Institutes of Health Research Grants P01CA85878, R24CA83099, and P50CA093990; and the Charles A. Dana Foundation. D.A.H. was the recipient of a Varian Medical Systems/Radiological Society of North America Holman Pathway Research Resident Seed Grant.

1. Behin, A., Hoang-Xuan, K., Carpentier, A. F. & Delattre, J. Y. (2003) *Lancet* **361,** 323–331.
2. Macdonald, D. R., Cascino, T. L., Schold, S. C., Jr., & Cairncross, J. G. (1990) *J. Clin. Oncol.* **8,** 1277–1280.
3. Barker, F. G., Prados, M. D., Chang, S. M., Gutin, P. H., Lamborn, K. R., Larson, D. A., Malec, M. K., McDermott, M. W., Sneed, P. K., Wara, W. M., *et al.* (1996) *J. Neurosurg.* **84,** 442–448.
4. Gaspar, L. E., Fisher, B. J., MacDonald, D. R., LeBer, D. V., Halperin, E. C., Schold, S. C., Jr., & Cairncross, J. G. (1993) *Int. J. Radiat. Oncol. Biol. Phys.* **25,** 877–879.
5. Wood, J. R., Green, S. B. & Shapiro, W. R. (1988) *J. Clin. Oncol.* **6,** 338–343.
6. Grant, R., Walker, M., Hadley, D., Barton, T. & Osborn, C. (2002) *J. Neurooncol.* **57,** 241–245.
7. Hess, K. R., Wong, E. T., Jaeckle, K. A., Kyritisis, A. P., Levin, V. A., Prados, M. D. & Yung, W. K. A. (1999) *Neuro–Oncol.* **1,** 282–288.
8. Grant, R., Liang, B. C., Slattery, J., Greenberg, H. S. & Junck, L. (1997) *Neurology* **48,** 1336–1340.
9. Ross, B. D., Chenevert, T. L., Kim, B. & Ben-Joseph, O. (1994) *Q. Magn. Reson. Biol. Med.* **1,** 89–106.
10. Chenevert, T. L., Stegman, L. D., Taylor, J. M., Robertson, P. L., Greenberg, H. S., Rehemtulla, A. & Ross, B. D. (2000) *J. Natl. Cancer Inst.* **92,** 2029–2036.
11. Hamstra, D. A., Lee, K. C., Tychewicz, J. M., Schepkin, V. D., Moffat, B. A., Chen, M., Dornfeld, K. J., Lawrence, T. S., Chenevert, T. L., Ross, B. D., *et al.* (2004) *Mol. Ther.* **10,** 916–928.
12. Hall, D. E., Moffat, B. A., Stojanovska, J., Johnson, T. D., Li, Z., Hamstra, D. A., Rehemtulla, A., Chenevert, T. L., Carter, J., Pietronigro, D. & Ross, B. D. (2004) *Clin. Cancer Res.* **10,** 7852–7859.
13. Rehemtulla, A., Hall, D. E., Stegman, L. D., Prasad, U., Chen, G., Bhojani, M. S., Chenevert, T. L. & Ross, B. D. (2002) *Mol. Imaging* **1,** 43–55.
14. Mardor, Y., Pfeffer, R., Spiegelmann, R., Roth, Y., Maier, S. E., Nissim, O., Berger, R., Glicksman, A., Baram, J., Orenstein, A., *et al.* (2003) *J. Clin. Oncol.* **21,** 1094–1100.
15. Moffat, B. A., Chenevert, T. L., Lawrence, T. S., Meyer, C. R., Johnson, T. D., Dong, Q., Tsien, C., Mukherji, S., Quint, D. J., Gebarski, S. S., *et al.* (2005) *Proc. Natl. Acad. Sci. USA* **102,** 5524–5529.
16. Chan, J. L., Lee, S. W., Fraass, B. A., Normolle, D. P., Greenberg, H. S., Junck, L. R., Gebarski, S. S. & Sandler, H. M. (2002) *J. Clin. Oncol.* **20,** 1635–1642.
17. Le Bihan, D., Breton, E., Lallemand, D., Aubin, M. L., Vignaud, J. & Laval-Jeantet, M. (1988) *Radiology* **168,** 497–505.
18. Pierpaoli, C., Jezzard, P., Basser, P. J., Barnett, A. & Di Chiro, G. (1996) *Radiology* **201,** 637–648.
19. Meyer, C. R., Boes, J. L., Kim, B., Bland, P. H., Zasadny, K. R., Kison, P. V., Koral, K., Frey, K. A. & Wahl, R. L. (1997) *Med. Image Anal.* **1,** 195–206.
20. Hastie, T., Tibshirani, I. & Friedman, J. (2001) *The Elements of Statistical Learning: Data Mining, Inference, and Prediction* (Springer, New York).
21. Bossuyt, P. M., Reitsma, J. B., Bruns, D. E., Gatsonis, C. A., Glasziou, P. P., Irwig, L. M., Lijmer, J. G., Moher, D., Rennie, D. & De Vet, H. C. W. (2003) *Clin. Radiol.* **58,** 575–580.
22. Curran, W. J., Jr., Scott, C. B., Horton, J., Nelson, J. S., Weinstein, A. S., Fischbach, A. J., Chang, C. H., Rotman, M., Asbell, S. O., Krisch, R. E., *et al.* (1993) *J. Natl. Cancer Inst.* **85,** 704–710.
23. Stupp, R., Mason, W. P., van den Bent, M. J., Weller, M., Fisher, B., Taphoorn, M. J., Belanger, K., Brandes, A. A., Marosi, C., Bogdahn, U., *et al.* (2005) *N. Engl. J. Med.* **352,** 987–996.
24. Hegi, M. E., Diserens, A. C., Gorlia, T., Hamou, M. F., de Tribolet, N., Weller, M., Kros, J. M., Hainfellner, J. A., Mason, W., Mariani, L., *et al.* (2005) *N. Engl. J. Med.* **352,** 997–1003.
25. Nutt, C. L., Mani, D. R., Betensky, R. A., Tamayo, P., Cairncross, J. G., Ladd, C., Pohl, U., Hartmann, C., McLaughlin, M. E., Batchelor, T. T., *et al.* (2003) *Cancer Res.* **63,** 1602–1607.
26. Cairncross, J. G., Ueki, K., Zlatescu, M. C., Lisle, D. K., Finkelstein, D. M., Hammond, R. R., Silver, J. S., Stark, P. C., Macdonald, D. R., Ino, Y., *et al.* (1998) *J. Natl. Cancer Inst.* **90,** 1473–1479.
27. Louis, D. N., Holland, E. C. & Cairncross, J. G. (2001) *Am. J. Pathol.* **159,** 779–786.
28. Sykova, E., Svoboda, J., Polak, J. & Chvatal, A. (1994) *J. Cereb. Blood Flow Metab.* **14,** 301–311.
29. Sinha, S., Lucas-Quesada, F. A., Sinha, U., De Bruhl, N. & Bassett, L. W. (2002) *J. Magn. Reson. Imaging* **15,** 693–704.
30. Kremser, C., Judmaier, W., Hein, P., Griebel, J., Lukas, P. & de Vries, A. (2003) *Strahlenther. Onkol.* **179,** 641–649.
31. Liapi, E., Kamel, I. R., Bluemke, D. A., Jacobs, M. A. & Kim, H. S. (2005) *J. Comput. Assist. Tomogr.* **29,** 83–86.
32. Sinha, S. & Sinha, U. (2004) *Magn. Reson. Med.* **52,** 530–537.
33. Wang, J., Takashima, S., Takayama, F., Kawakami, S., Saito, A., Matsushita, T., Momose, M. & Ishiyama, T. (2001) *Radiology* **220,** 621–630.
34. Theilmann, R. J., Borders, R., Trouard, T. P., Xia, G., Outwater, E., Ranger-Moore, J., Gillies, R. J. & Stopeck, A. (2004) *Neoplasia* **6,** 831–837.
35. Takahara, T., Imai, Y., Yamashita, T., Yasuda, S., Nasu, S. & Van Cauteren, M. (2004) *Radiat. Med.* **22,** 275–282.